Repetitive Trans Spinal Magnetic Stimulation Improves Functional Recovery and Tissue Repair in Contusive and Penetrating Spinal Cord Injury Models in Rats

Amandine Robac
Université de Rouen Normandie - EA3830
Pauline Neveu
Université de Rouen Normandie -EA3830
Alizée Hugede
Université de Rouen Normandie - EA3830
Elisabeth Garrido
Université de Rouen Normandie - EA3830
Lionel Nicol
Université de Rouen Normandie - U1096
Quentin Delarue
Université de Rouen Normandie - EA3830
Nicolas Guérout (nicolas.guerout@univ-rouen.fr)
Universite de Rouen UFR Santé de Rouen

Research

Keywords: rehabilitation, spinal cord injury, glial scar, magnetic stimulation, cystic cavities and functional recovery.

Posted Date: October 27th, 2021

DOI: https://doi.org/10.21203/rs.3.rs-1002347/v1

Version of Record: A version of this preprint was published at Biomedicines on December 3rd, 2021. See the published version at https://doi.org/10.3390/biomedicines9121827.

Abstract

Spinal cord injury (SCI) is an incurable condition in which the brain is disconnected partially or completely from the periphery. Mainly SCI are traumatic and are due to traffic, domestic or sport accidents. To date SCI are incurable and let, most of the time, the patients with a permanent loss of sensitive and motor functions. Therefore, since several decades researchers tried to develop treatments to cure SCI. Among them, recently, our lab have demonstrated that in mice, repetitive trans-spinal magnetic stimulation (rTSMS) can, after SCI, modulate the lesion scar and can induce functional locomotor recovery non-invasively. These results are promising, however before to translate them to Humans it is important to reproduce them in a more clinically relevant model. Indeed, SCI do not lead to the same cellular events in mice and Humans. In particular, SCI in Humans induce the formation of cystic cavities. That is why we propose here to validate the effects of rTSMS in rat, animal model in which SCI lead to the formation of cystic cavities, after penetrating and contusive SCI. To do so, several techniques including immunohistochemical, behavioral and MRI have been performed. Our results demonstrate that rTSMS, in both SCI models, modulates the lesion scar by decreasing the formation of cystic cavities and by improving axonal survival. Moreover, rTSMS, in both models, enhances functional locomotor recovery.

Altogether, our study describes that rTSMS exerts positive effects after SCI in rats. This study is a further step towards the use of this treatment in Humans.

Introduction

Spinal cord injury (SCI) is a debilitating condition which can lead to a permanent loss of motor and sensitive functions. To date, there is no curative treatment which can be proposed to injured patients. That is why fundamental and preclinical studies have been conducted since several decades to find out innovative therapies [1]. Researches have followed different paths, the first one tried to modulate the inhibitory microenvironment presents after SCI and the second one harnessed to replace the lost cells such as neurons or oligodendrocytes [2]. These two strategies are based on the knowledge acquired about the cellular and molecular events that take place after SCI. Indeed, at cellular level, SCI induces a massive inflammation with the infiltration of circulating immune cells such as macrophages and induction of microglia reactivity [3]. At the same time the initial traumatic injury leads to neuronal and oligodendroglial death [2,4]. Altogether, these cellular events conduct to the formation of a spinal scar composed of a fibrotic core presents into the lesion epicenter and of an astroglial scar located at the border of the lesion [5–7]. This spinal scar exerts complementary and opposite effects. In fact, it segregates the inflammatory cells to avoid the expansion of the lesion but also inhibit axonal regrowth. In effect, the spinal scar secretes a wide range of extracellular matrix molecules including chondroitin sulfate proteoglycan, a class of molecules known as one of the major inhibitory components of the lesion scar [8]. To alleviate this inhibitory microenvironment we and other research groups have assessed the effects of different therapies such as cellular transplantation, biomaterials' graft or more recently repetitive magnetic stimulation [9–13]. To do so, rodent's models have been massively used, mainly mice and rats. However, it

is important to note that the cellular events and also the composition of the spinal scar which take place after SCI are distinct between mice and rats but also with Humans. In effect, in rats and Humans, the fibrotic core presents at the lesion epicenter of the spinal scar in mice is replaced progressively by cystic cavities within weeks to months after SCI [14]. That is why it can be of primary importance before to translate an innovative therapy to clinical in Humans to validate it in mice and also in rats. In a clinical related perspective it is also important to mimic the lesion which occurs in Humans. Indeed, in Humans SCI are mainly due to contusive injury whereas in preclinical models, SCI are oftenly penetrating because this model is reproducible and does not require specific apparatus [15].

Recently, our research group reports that repetitive trans-spinal magnetic stimulation (rTSMS) can be used as a non-invasive treatment after SCI. Our study demonstrates that rTSMS modulates the spinal scar, enhances axonal regrowth and locomotor recoveries [9,16,17]. These experiments have been conducted in a mouse model and SCI have been performed by complete transection. That is why, we propose here to validate this promising therapy in a rat model. Our work has been conducted in both penetrating and contusive SCI in a large cohort of 104 rats.

Materials And Methods

Animal care and use statement

The protocols were designed to minimize pain or discomfort to the animals. All experimental procedures were in accordance with the European Community guiding principles on the care and use of animals (86/609/CEE; Official Journal of the European Communities no. L358; December 18, 1986), French Decree no. 97/748 of October 19, 1987 (Journal Officiel de la République Française; October 20, 1987), and the recommendations of the Cenomexa ethics committee (#23767).

Experiments were performed on adult Sprague Dawley female rats (Janvier Labs, Le Genest-Saint-Isle, France) at eight–ten weeks of age (average weight 260 – 280g).

Female rats were housed (two rats/cage) in secure conventional rodent facilities on a 12-hr light/dark cycle with constant access to food and water.

Our two procedures were composed of two main experimental groups:

SCI control group: animals received SCI.

SCI + STM group: animals received SCI and rTSMS treatment during 15 days.

For the two procedures histological analyses have been performed at 15 and 60 days after SCI. Functional analyses including plantar and locotronic tests have been performed at 15, 30 and 60 days after SCI.

For the second procedure only (contusive SCI), MRI experiments have been performed at 7, 21 and 42 days after SCI.

A total of 104 rats have been included in the entire study (procedure 1 and procedure 2).

A general overview of these experiments is presented in Figure 1.

Experimental design

Procedure 1

Surgical procedure

In order to assess the effects of the rTSMS treatment and to compare them to those described in mice, first we performed penetrating SCI in rats [9,16].

To do so, rats received 30 min before surgery a subcutaneous injection of buprenorphine hydrochloride (0,3 mg/mL). Then, rats were anesthetized with 2% of isofluorane during the entire surgery (Iso-Vet, Osalia, Paris, France). Animal's body temperature has been kept steady at 37°C with a heating pad during entire surgical intervention. After being shaved and disinfected with betadine solution, the dorsal skin of the rats was incised, the superficial fat gently shifted, and the muscle tissue dissected to expose laminae T9–T11. Posterior part of vertebrae was countersank in order to create an ample space for lesion. SCI were performed at T10 level as described previously [9,16]. After laminectomy, the dura mater was removed and a complete transection of the spinal cord was performed with 25-gauge needle. After surgery, rats underwent daily check, none of them showed neither skin lesion, infection, nor autophagy throughout the study.

For this procedure 56 rats have been used (Figure 1):

- 2 groups of 8 rats for the immunohistological experiments 15 days after SCI

- 2 groups of 20 rats for functional tests and for immunohistological experiments 60 days after SCI

Procedure 2

Surgical procedure

In Humans, SCI are mainly due to contusive injuries, thus in a second time we investigated the effects of rTSMS in a contusion model in rats. A moderate/severe lesion model has been chosen due to the fact that 60% of the lesions in Humans are incomplete [14].

The surgery was performed as described above except for the lesion step.

Indeed, after laminectomy, the dura mater was removed and contusion injury was applied using a force-controlled spinal cord impactor (IH-0400 Impactor, Precision Systems and Instrumentation LLC, USA). The applied force was set to 175 kdyn. The spinal cord displacement induced by the impact was measured for each animal. After surgery, rats underwent daily check, none of them showed neither skin lesion, infection, nor autophagy throughout the study.

For this procedure 56 rats have been used as described above for the procedure 1 (Figure 1).

rTSMS treatment

rTSMS was delivered with a commercially available figure of eight double coil featuring an air cooling system connected to a Magstim rapid2 stimulator used for focal cortical and peripheral stimulations (Magstim, Whitland, UK). The coil was positioned in close contact with the back of the animal at the site of injury. The size of the area stimulated has been defined according to the manufacturer's device manual. The area stimulated was 1.5 cm^2. The position of the coil was maintained using an articulated arm stand. The exact position of the coil was defined using the mark located in the middle of the coil. rTSMS treatment was applied at a frequency of 10 Hz, 10 min per day during 14 days. Stimulation protocol consisted of 10 s stimulation followed by 20 s of rest. Rats were kept under anesthesia with 2% of isoflurane during stimulation; the equivalent anesthesia were used for untreated animals. Peak magnetic intensity at the experimental distance was 0.4 T.

Functional test

Locotronic test: Foot misplacement apparatus

Experiments have been performed as described previously by Chalfouh et al. (Intellibio, Nancy,

France) [9]. The equipment consists of a flat ladder on which the animal can move from the starting zone towards the arrival zone. On both sides of the ladder, infrared sensors allow the visualization and recording of the displacement of the animal. The location and precise length of time of all the errors are recorded, in distinguishing the errors from front legs, back legs and tail. Based on all data recorded; number of back legs errors, total back legs errors time and total crossing time were provided by the software and compared between groups of animals.

All the rats were pre-trained on the ladder, one week prior to injury to provide baseline data.

Hargreaves apparatus

The Hargreaves test instrument used in this study was a plantar test (Ugo Basile, Italy). A radiative heat source was placed beneath the animal and pointed at the plantar surface of the hindpaw. The time

between the onset of the thermal radiation stimulus and the appearance of paw withdrawal was recorded as the hindpaw withdrawal thermal latency [18]. Baseline parameters have been obtained with an additional group of non-injured animals.

MRI Imaging

In-vivo imaging experiment were performed on rat to follow on the same rats the evolution of the spinal cord structure overtime after SCI. Analysis of the spinal cord structure was achieved by the MRI BioSpec Advanced II (Bruker, Germany), with a magnetic field of 4.7 Teslas, monitored with ParaVision software.

The rats were anesthetized by intraperitoneal injections (Thiopental, 1g/20mL, Panpharma). To perform the MRI recordings, the rats were placed in supine position. The vertebra T9 was putted down on the marker of the antenna in order to have the area of interest in the field of view of the MRI. Two cardiac electrodes were placed on the rats to follow their cardiac constants.
A comprehensive analysis including T2*-weighted gradient echo, in axial and sagittal sections, was carried out with the parameters presented in the Table.1.

The sequence performed on axial sections is a multi-slice gradient which allowed to provide a T2* map for tissues characterization.

The sequences of images were then analyzed through the:

- ParaVision software, to determine the surface quantization of hyposignal and hypersignal, but also identify tissues structure on sagittal images;
- Osirix software, to determine the volume of spinal cord section and realize a 3D representation on axial images.

Tissue preparation and sectioning

Animals were deeply anesthetized with sodium pentobarbital (120mg/kg body weight) and perfused transcardially with PBS followed by ice-cold 4% formaldehyde in PBS. Dissected spinal cords were further post-fixed in 4% PFA in PBS at 4 °C overnight and cryoprotected in

30% sucrose (Life Technologies, Carlsbad, CA) for at least 48 h. After embedding in Tissue-

Tek OCT compound (Sakura, Tokyo, Japan), the spinal cords were cut sagittally to 20 µm thickness. Sections were collected accordingly to stereological principles (five sections per slide) and stored at −20 °C until further use.

Immunohistochemistry

Spinal cord sections were blocked with 10% Normal Donkey serum (Jackson ImmunoResearch, Cambridge, UK), 0.3% Triton-X100 (Sigma-Aldrich) in PBS, then incubated overnight at room temperature in a humidified chamber with primary antibodies diluted in blocking solution. The following primary antibodies were used: Rabbit anti-Platelet-derived growth factorβ (PDGFRβ, Abcam, ab32570), Mouse anti-Glial fibrillary acidic protein (GFAP Cy3-conjugated Sigma-Aldrich, C9205 and GFAP unconjugated Sigma-Aldrich, G3893), Rabbit anti-ionized calcium-binding adapter molecule 1 (Iba1, Wako, 019-19741, Osaka, Japan) and Mouse anti-neurofilament 200kD (NF200, Millipore, MAB5256).

After washing, antibody staining was revealed using species-specific fluorescence-conjugated secondary antibodies (Jackson ImmunoResearch). Sections were counterstained with 4',6-diamidino-2-phénylindole (DAPI; 1 µg/mL; Sigma-Aldrich) and coverslipped with Vectashield mounting media (Vector Labs, Burlingame, UK).

Image acquisition analysis

Representative images of the lesion site and spinal cords were acquired using the Zeiss Apotome2 microscope set up. For tissue analysis sagittal sections have been used. For each experimental group and staining, 6 to 17 animals were analyzed. The image processing and assembly was acquired with Image J software.

Quantification of immunohistochemically stained areas

On sagittal sections, the GFAP negative (GFAP-), PDGFRβ positive (PDGFRβ+), NF200 negative (NF200-) and DAPI negative (DAPI-) areas were measured at the epicenter of the lesion and section rostral and caudal to the injury site, thus a minimum of 3 sections (60µm) per animal have been measured. For Iba1 staining, analysis of the area in which Iba1 positive amyboid cells were present has been measured. Analysis of Iba1 intensity measurement was performed on rectangle of 6 µm × 2 µm. Iba1 intensities were collected after threshold standardization.

Statistical analysis

Data are presented as means ± standard deviation (SD). Comparison of means were performed using two-tailed Mann-Whitney tests for all the experiments. In all tests, $P < 0.05$ were considered statically significant.

Results

Procedure 1

The main aim of the first procedure was to investigate the effects of rTSMS after a complete transection of the spinal cord in rats. We focused this study on functional recovery and tissue repair (Figure 1).

rTSMS treatment induces locomotor recovery after a complete transection of the spinal cord in rats

Based on locotronic and Hargreaves tests, motor and sensitive recoveries have been assessed respectively.

Hargreaves test results demonstrate that there is no difference between groups at 15, 30 and 60 days after SCI (Figure S1).

Locotronic results demonstrate that 15 days after SCI, rTSMS treatment did not enhance locomotor abilities (Figure 2A-C), indeed there is no significant difference between SCI and Stm groups at this time point (Figure 2A-C). At the opposite, 30 days and 60 days after SCI, rTSMS treated animals show a significant improvement of the locomotion (Figure 2 D-I). In fact, Stm group presents a reduction of the number of back legs errors (Figure 2D and G), the total back legs errors' time (Figure 2E and H) and total crossing time (Figure 2Fand I) 30 and 60 days after SCI.

rTSMS treatment enhances tissue repair after a complete transection of the spinal cord in rats

In order to investigate the effects of rTSMS on tissue repair, immunohistological experiments have been performed 15 and 60 days after SCI (Figures 3 and 4 respectively).

Glial and fibrotic components of the scar have been studied (Figure 3 A-H). It appears that 15 days after SCI, rTSMS treatment reduces the fibrotic component of the scar (Figure 3H) but has no major effect at this time point on the glial component of the scar (Figure 3G). In contrast, 60 days after SCI, our results reveal that rTSMS modulates the spinal scar by decreasing the GFAP negative (GFAP-) area (Figure 4G). At this time point rTSMS does not exert major effect on the fibrotic component of the scar (Figure 4H).

In rats, one of the main issue after SCI is the presence of cystic cavities which take place into the epicenter of the lesion. To measure this process, DAPI negative (DAPI-) area has been assessed at 15 and 60 days after SCI. 15 days after SCI, there is no difference between the two groups of animals (Figure 3L, I and O), whereas at 60 days, rTSMS tends to decrease the size of the cavities (P=0.1135) (Figure 4L, I and O).

After SCI, neuronal death and axonal degeneration impair functional recovery, that is why 15 and 60 days after SCI axonal quantification has been investigated *via* NF200 staining. Our results show that at both time points; 15 days (Figure 3J, M and P) and 60 days after SCI (Figure 4J, M and P) rTSMS treatment decreases the NF200 negative (NF200-) area.

Finally, inflammatory processes have been investigated 15 and 60 days after SCI. Indeed, inflammation and reactivity of the immune cells mainly microglia and macrophages are key factors regulating tissue healing. Thus, reactivity of microglia/macrophages has been assessed using Iba1 staining. These

measurements reveal that 15 days (Figure 3R, U and W) and 60 days (Figure 4R, U and W) after SCI, rTSMS treatment decreases the amount of amyboid Iba1 positive cells into the injured spinal cord parenchyma. Iba1 intensity has been also assessed and did not show any difference between groups 15 and 60 days after SCI (Figure 3X and 4X).

Procedure 2

The main aim of this second procedure was to investigate the effects of rTSMS after a moderate/severe contusion of the spinal cord in rats. In addition to functional recovery and tissue repair, MRI analyses have been performed (Figure 1).

rTSMS treatment induces functional recovery after contusive SCI in rats

First, sensitive recovery has been investigated. To do so, hind paw withdrawal thermal latency has been measured using Hargreaves plantar test 15, 30 and 60 days after SCI (Figure 5). These experiments show that at 15, 30 and 60 after SCI rTSMS treated animals presented a reduction of the hindpaw withdrawal thermal latency in comparison to untreated (SCI) animals (Figure 5A-C).

Then, based on locotronic test, functional recoveries have been assessed. Our results demonstrate that 15 and 30 days after SCI, rTSMS treatment did not enhance locomotor abilities (Figure 6A-F), indeed there is no significant difference between SCI and Stm groups at this time points (Figure 6A-F). More interestingly, 60 days after SCI, rTSMS treated animals show a significant improvement of the locomotion (Figure 6G-I). Indeed, Stm group presents a reduction of the number of back legs errors (Figure 6G), total back legs errors time (Figure 6H) and total crossing time (Figure 6I) 60 days after SCI.

MRI analyses show that rTSMS treatment decreases cystic cavities and increases spinal cord spared tissue

MRI experiments have been performed at 7 (Figure 7A-F), 21 (Figure 7G-L) and 42 (Figure 7M-R) days after SCI in order to follow on the same rats the evolution of the injury site overtime after SCI and rTSMS treatment. Hyposignal measurement was representative of the fibrotic/necrotic tissue presents into the parenchyma, whereas hypersignal indicates the presence of inflammation at early time points (7 and 21 days, Figure 7A-L) and cystic cavities at later time point (42 days, Figure 7M-R). Measurement of both hypo and hypersignal has been also performed, it reflects the overall area of the injured tissue (Figure 7E, K and Q). Based on this overall area measurement, a ratio of lesioned tissue among the entire spinal cord parenchyma has been calculated (Figure 7F, L and R).

The MRI analyses reveal that 7 and 21 days after SCI there is no difference between groups (Figure 7A-L). In contrast, 42 days after SCI, rTSMS treated animals presented a reduction of the hypersignal area (Figure 7M, N and P), the overall area of the injured tissue (Figure 7Q) and the ratio of lesioned tissue (Figure 7R).

rTSMS treatment enhances tissue repair after contusive SCI in rats 60 days after SCI.

In order to investigate the effects of rTSMS on tissue repair, immunohistological experiments have been performed 15 and 60 days after SCI (Figures 8 and 9 respectively).

In this model, in the same way that MRI results, immunohistological analyses demonstrate that 15 days after SCI there is no difference between treated (Stm) and untreated (SCI) animals (Figures 8).

At the opposite, 60 days after SCI, the analysis of the glial and fibrotic components of the scar show that rTSMS treatment decreases the GFAP negative area without decreasing PDGFRβ positive area (Figure 9A-H). In the same way, at this time point, rTSMS treatment decreases cystic cavities (DAPI negative area) and axonal degeneration (NF200 negative area) (Figure 9I, L and O and JM and P respectively). Moreover, rTSMS treated group presents an increase of the amount of amyboid Iba1 positive cells (Figure 9R, U and W). Iba1 intensity has been also assessed and did not show any difference between groups 60 days after SCI (Figure 9X).

Discussion

The main aim of our study was to investigate the effects of rTSMS in penetrating and contusive SCI models in rats (Figure1). Indeed, the effects of rTSMS have been measured first in a penetrating injury model in which the spinal cord was transected with a needle. This model has been chosen because it was used initially in our princeps studies in mice [9,16]. As described in mice, in this model, rTSMS treatment enhances functional recovery and modulates the lesion scar in rats. In effect, 15 days after SCI, treated rats present a reduction of the fibrotic scar and an increase of the axonal survival (reduction of NF200 negative area) (Figure 3). These effects on tissue repair are correlated with functional recovery at later time points; 30 and 60 days after SCI (Figure 2). Finally, 60 days after SCI, treated animals present an improvement of the repair of the spinal cord by the decrease of the size of the cavities and the increase of the glial scar (Figure 4).

In a second time we assessed the effects of rTSMS in a more clinically relevant model. Indeed, the vast majority of the SCI in Humans are contusive and not penetrating [19]. For this procedure, a moderate/severe contusive SCI model has been chosen because in Humans 60% of the SCI are not complete [19]. This model induces a severe histological injury characterized by large cystic cavities and moderate locomotor deficits. This procedure complete the first one in which the animals present in addition to a severe histological injury, a complete paraplegia. To do so, standardized contusive SCI have been performed using a force-controlled spinal cord impactor. In this model, it appears that rTSMS improves also functional recovery and tissue repair. More interestingly, our results indicate that in this model, rTSMS treatment has a major effect at later time point. In fact, rTSMS treated animals present a significant functional recovery only 60 days after SCI (Figure 6). In the same way, histological analyses reveal that 15 days after SCI there is no difference between the two groups of rats whereas 60 days after SCI, treated animals show a reduction of the size of the cavities and an increase of the glial scar and the neuronal survival (Figures 8 and 9). In addition to these analyses, MRI experiments have been also performed 7, 21 and 42 days after SCI (Figure 7). These experiments confirm our histological results. In

effect, 7 and 21 days after SCI there is no difference between the two groups of rats. At the opposite, 42 days after SCI, MRI results show that rTSMS treated animals present a reduction of the hypersignal - corresponding to the cavities -, the hyper and hyposignal - corresponding to the lesioned tissue - and the ratio of lesioned tissue among the entire spinal cord parenchyma (Figure 7).

Ultimately, in our study we tried to evaluate the sensitive recovery after SCI. Indeed, plantar test has been performed in both groups of animals and in both procedures, 15, 30 and 60 days after SCI (Figure 1). Based on that test, hindpaw withdrawal thermal latency has been recorded. In procedure 1 (penetrating SCI), plantar test results did not show any difference between groups (Figure S1). In contrast, in procedure 2 (contusive SCI) it appears that rTSMS treated animals present a reduction of hindpaw withdrawal thermal latency recordings for all time points in comparison to untreated animals (Figure 5). More interestingly, a closer analysis of these results allows to see that at 15 days after SCI, hindpaw withdrawal thermal latency recordings of the rTSMS treated animals is shorter in comparison to non-injured animals (dashed line, Figure 5A). At the opposite, at later time points, 30 and 60 days after SCI, hindpaw withdrawal thermal latency recordings of the rTSMS treated animals is comparable to the one of non-injured animals (dashed lines, Figure 5B and C). These results can illustrate the fact that at early time-point (15 days) rTSMS treatment induces allodynia, due to the shorter latency than non-injured animals, whereas at later time-points (30 and 60 days after SCI) rTSMS enhances axonal survival and reestablishes an efficient voluntary sensitive-motor loops close to those of the uninjured rats. Allodynia is a commonly described side-effect of several therapies after SCI such as cellular transplantation. In effect, cellular transplantation plays its presumed effects mainly by replacing lost cells or by secreting trophic factors which increase axonal survival or axonal regrowth. These benefits can in turn exert detrimental side-effects such as neuropathic pain or allodynia [20,21]. We can hypothesize that at early time point after contusive SCI, rTSMS enhances allodynia at least in case of thermoalgic stimulations due to enhancement of axonal survival and that at later time points this axonal survival induces neuronal plasticity in reorganizing functional sensitive-motor loops networks. The reduction of hindpaw withdrawal thermal latency recordings in comparison to uninjured animals is also observed after penetrating SCI in both groups for all time points studied (Figure S1).

Our two procedures allow also to characterize the evolution of the lesion scar overtime. Indeed, immunohistological results demonstrate that in both cases, at 15 days after SCI the scar is composed of a diffuse (after contusive SCI) or a dense (after penetrating SCI) fibrotic core. At this time point, there is only rare cystic cavities. In contrast, 60 days after SCI, in both cases, there is no or very few fibrotic scar, however the spinal cord presents very large cystic cavities. These results are especially interesting because the lesion scar in rats 15 days after SCI is comparable to the one presents in mice [22,23]. While, at 60 days after SCI the two scars are very different due to the fact that the fibrosis present in rats degenerates to the detriment of the cystic cavities which is not the case in mice models. It appears, that further studies will be necessary to understand the mechanisms responsible of this distinct lesion scar evolution overtime. In a broader perspective, it has been recently shown that this fibrotic scar is present in different central nervous system lesions in mice such as traumatic brain or spinal cord injuries but also

after demyelinating or ischemic lesion models [24]. It could be also interesting to demonstrate if this fibrotic scar is present throughout species after CNS lesions.

Recent studies have underlined the major role played by microglia/macrophages after SCI [25,26]. That is why, we have investigated the effects of rTSMS treatment on these cellular populations. To do so, Iba1 staining experiments have been performed. In particular, Iba1 intensity has been measured and, in both procedures and both time points investigated, it appears that there is no difference between groups. To complete this analysis, we quantified the amyboid Iba1 positive cells areas present into the lesion epicenter. These analyses show that in penetrating SCI (procedure 1), rTSMS treatment decreases the amount of amyboid Iba1 positive cells areas at both time points. In contrast, in contusive SCI (procedure 2), the analyses show that rTSMS treatment increases the amount of the amyboid Iba1 positive cells areas at 60 days after SCI. The amyboid shape quantification is usually employed to characterize the activation of microglia and macrophages [27]. Altogether, our results underline the fact that rTSMS treatment modulates microglia/macrophages activation and inflammatory response. However, the opposite results on Iba1 positives cells in our two procedures do not allow to conclude about the specific effects of rTSMS on these cellular populations. Recent studies have demonstrated that circulating macrophages are mostly present into the lesion core whereas microglia are present at the border of it [25]. It has been also shown that macrophages instead of microglia are mainly implicated in secondary axonal dieback ([28]. The immunomodulatory role played by magnetic stimulation (MS) on macrophages in culture has been already investigated ([29]. It appears that MS can act on macrophages polarization. However, the precise role of MS and especially rTSMS on microglia and macrophages *in vivo* after SCI is not clearly described. It could be of primary interest to conduct further investigations regarding the polarization of microglia/macrophages after rTSMS treatment. Single cell sequencing could be a useful technic to reveal the diversity of the inflammatory cells present into the lesioned spinal cord with or without rTSMS treatment. Some recent studies have pointed the fact that there is specific microglial subpopulations associated to neurodegenerative diseases [30,31]. This kind of studies could be performed in order to characterize the role played by rTSMS on microglia/macrophages and by extension on the other inflammatory cells.

The main aim of the present research was to propose a preclinical study based on two complementary SCI models. Thus, its main limitation is that our study does not dissect the cellular and molecular mechanisms which can explain the role played by rTSMS after SCI. However, our study describes that rTSMS exerts positive effects after SCI in rats, animal model in which the consequences of SCI are closer to the ones observed in Humans. This study is a further step towards the use of this treatment in Humans after SCI.

Declarations

Acknowledgements

Behavioural studies and processing were conducted with the support of equipment from the Behavioural Analysis Platform SCAC (University of Rouen Normandy, France).

Authors' Contributions

N.G. conceptualized the project. N.G. designed the experiments. A.R., P.N., A.H., E.G., and L.N performed the experiments. A.R., P.N., A.H., E.G., Q.D. and N.G. analyzed the results. Q.D. provided techniques and scientific input. A.R., P.N., A.H. and N.G. wrote the article.

All authors read and approved the final manuscript.

Funding

This research was supported by ADIR association (ADIR-2019-03), IRME association, fonds de dotation Neuroglia (REGENrTSMS) and Fondation de l'Avenir (AP-RM-20-028).

Availability of supporting data

The authors confirm that the data supporting the findings of this study are available within the article and its Supplement material.

Consent for publication

All authors have read the manuscript and indicated consent for publication

Competing interests

The authors declare that they have no competing interests.

References

1. Guérout N. Plasticity of the Injured Spinal Cord. *Cells*. 2021;10(8):1886. doi:10.3390/cells10081886
2. Hejrati N, Fehlings MG. A review of emerging neuroprotective and neuroregenerative therapies in traumatic spinal cord injury. *Curr Opin Pharmacol*. 2021;60:331-340. doi:10.1016/j.coph.2021.08.009
3. Brockie S, Hong J, Fehlings MG. The Role of Microglia in Modulating Neuroinflammation after Spinal Cord Injury. *Int J Mol Sci*. 2021;22(18):9706. doi:10.3390/ijms22189706
4. Grégoire C-A, Goldenstein BL, Floriddia EM, Barnabé-Heider F, Fernandes KJL. Endogenous neural stem cell responses to stroke and spinal cord injury. *Glia*. 2015;63(8):1469-1482. doi:10.1002/glia.22851
5. Göritz C, Dias DO, Tomilin N, Barbacid M, Shupliakov O, Frisén J. A pericyte origin of spinal cord scar tissue. *Science*. 2011;333(6039):238-242. doi:10.1126/science.1203165
6. Sabelström H, Stenudd M, Frisén J. Neural stem cells in the adult spinal cord. *Exp Neurol*. 2014;260:44-49. doi:10.1016/j.expneurol.2013.01.026

7. Sabelström H, Stenudd M, Réu P, et al. Resident neural stem cells restrict tissue damage and neuronal loss after spinal cord injury in mice. *Science*. 2013;342(6158):637-640. doi:10.1126/science.1242576
8. Hussein RK, Mencio CP, Katagiri Y, Brake AM, Geller HM. Role of Chondroitin Sulfation Following Spinal Cord Injury. *Front Cell Neurosci*. 2020;14:208. doi:10.3389/fncel.2020.00208
9. Chalfouh C, Guillou C, Hardouin J, et al. The Regenerative Effect of Trans-spinal Magnetic Stimulation After Spinal Cord Injury: Mechanisms and Pathways Underlying the Effect. *Neurotherapeutics*. 2020;17(4):2069-2088. doi:10.1007/s13311-020-00915-5
10. Chedly J, Soares S, Montembault A, et al. Physical chitosan microhydrogels as scaffolds for spinal cord injury restoration and axon regeneration. *Biomaterials*. 2017;138:91-107. doi:10.1016/j.biomaterials.2017.05.024
11. Delarue Q, Mayeur A, Chalfouh C, et al. Inhibition of ADAMTS-4 Expression in Olfactory Ensheathing Cells Enhances Recovery after Transplantation within Spinal Cord Injury. *J Neurotrauma*. 2020;37(3):507-516. doi:10.1089/neu.2019.6481
12. Kobashi S, Terashima T, Katagi M, et al. Transplantation of M2-Deviated Microglia Promotes Recovery of Motor Function after Spinal Cord Injury in Mice. *Mol Ther*. 2020;28(1):254-265. doi:10.1016/j.ymthe.2019.09.004
13. Luo Y, Fan L, Liu C, et al. An injectable, self-healing, electroconductive extracellular matrix-based hydrogel for enhancing tissue repair after traumatic spinal cord injury. *Bioact Mater*. 2022;7:98-111. doi:10.1016/j.bioactmat.2021.05.039
14. Courtine G, Sofroniew MV. Spinal cord repair: advances in biology and technology. *Nat Med*. 2019;25(6):898-908. doi:10.1038/s41591-019-0475-6
15. Watzlawick R, Rind J, Sena ES, et al. Olfactory Ensheathing Cell Transplantation in Experimental Spinal Cord Injury: Effect size and Reporting Bias of 62 Experimental Treatments: A Systematic Review and Meta-Analysis. *PLoS Biol*. 2016;14(5):e1002468. doi:10.1371/journal.pbio.1002468
16. Delarue Q, Robac A, Massardier R, Marie J-P, Guérout N. Comparison of the effects of two therapeutic strategies based on olfactory ensheathing cell transplantation and repetitive magnetic stimulation after spinal cord injury in female mice. *J Neurosci Res*. 2021;99(7):1835-1849. doi:10.1002/jnr.24836
17. Delarue Q, Chalfouh C, Guérout N. Spinal cord injury: can we repair spinal cord non-invasively by using magnetic stimulation? *Neural Regen Res*. 2021;16(12):2429-2430. doi:10.4103/1673-5374.313033
18. Zhang Y, Ma S, Ke X, et al. The mechanism of Annexin A1 to modulate TRPV1 and nociception in dorsal root ganglion neurons. *Cell Biosci*. 2021;11(1):167. doi:10.1186/s13578-021-00679-1
19. Algahtany M, McFaull S, Chen L, et al. The Changing Etiology and Epidemiology of Traumatic Spinal Injury: A Population-Based Study. *World Neurosurg*. 2021;149:e116-e127. doi:10.1016/j.wneu.2021.02.066
20. Hofstetter CP, Holmström NAV, Lilja JA, et al. Allodynia limits the usefulness of intraspinal neural stem cell grafts; directed differentiation improves outcome. *Nat Neurosci*. 2005;8(3):346-353.

doi:10.1038/nn1405

21. Nakhjavan-Shahraki B, Yousefifard M, Rahimi-Movaghar V, et al. Transplantation of olfactory ensheathing cells on functional recovery and neuropathic pain after spinal cord injury; systematic review and meta-analysis. *Sci Rep*. 2018;8(1):325. doi:10.1038/s41598-017-18754-4
22. Soderblom C, Luo X, Blumenthal E, et al. Perivascular fibroblasts form the fibrotic scar after contusive spinal cord injury. *J Neurosci*. 2013;33(34):13882-13887. doi:10.1523/JNEUROSCI.2524-13.2013
23. Zhu Y, Soderblom C, Krishnan V, Ashbaugh J, Bethea JR, Lee JK. Hematogenous macrophage depletion reduces the fibrotic scar and increases axonal growth after spinal cord injury. *Neurobiol Dis*. 2015;74:114-125. doi:10.1016/j.nbd.2014.10.024
24. Dias DO, Kalkitsas J, Kelahmetoglu Y, et al. Pericyte-derived fibrotic scarring is conserved across diverse central nervous system lesions. *Nat Commun*. 2021;12(1):5501. doi:10.1038/s41467-021-25585-5
25. Bellver-Landete V, Bretheau F, Mailhot B, et al. Microglia are an essential component of the neuroprotective scar that forms after spinal cord injury. *Nat Commun*. 2019;10(1):518. doi:10.1038/s41467-019-08446-0
26. Li Y, Ritzel RM, Khan N, et al. Delayed microglial depletion after spinal cord injury reduces chronic inflammation and neurodegeneration in the brain and improves neurological recovery in male mice. *Theranostics*. 2020;10(25):11376-11403. doi:10.7150/thno.49199
27. Brifault C, Gras M, Liot D, May V, Vaudry D, Wurtz O. Delayed pituitary adenylate cyclase-activating polypeptide delivery after brain stroke improves functional recovery by inducing m2 microglia/macrophage polarization. *Stroke*. 2015;46(2):520-528. doi:10.1161/STROKEAHA.114.006864
28. Evans TA, Barkauskas DS, Myers JT, et al. High-resolution intravital imaging reveals that blood-derived macrophages but not resident microglia facilitate secondary axonal dieback in traumatic spinal cord injury. *Exp Neurol*. 2014;254:109-120. doi:10.1016/j.expneurol.2014.01.013
29. Vinhas A, Almeida AF, Gonçalves AI, Rodrigues MT, Gomes ME. Magnetic Stimulation Drives Macrophage Polarization in Cell to-Cell Communication with IL-1β Primed Tendon Cells. *Int J Mol Sci*. 2020;21(15):E5441. doi:10.3390/ijms21155441
30. Li Y, He X, Kawaguchi R, et al. Microglia-organized scar-free spinal cord repair in neonatal mice. *Nature*. 2020;587(7835):613-618. doi:10.1038/s41586-020-2795-6
31. Olah M, Menon V, Habib N, et al. Single cell RNA sequencing of human microglia uncovers a subset associated with Alzheimer's disease. *Nat Commun*. 2020;11(1):6129. doi:10.1038/s41467-020-19737-2

Tables

Table 1: Summary table of the acquisition parameters of MRI sequences used to characterize and identify spinal cord structure on rats after SCI and/or rTSMS treatment.

	TR (msec)	*TE (msec)*	*Thickness (μm)*	*FOV (cm)*	*Matrix (pixel)*	*Acquisition time*
T2-weighted axial section*	2000	6.5 20.4 34.3 48.1 62.1 75.9 89.1 103.7 117.5 131.4	500	4	256	15 min 56s
T2-weighted saggital section*	2000	6.5	500	4	320	16 min

Figures

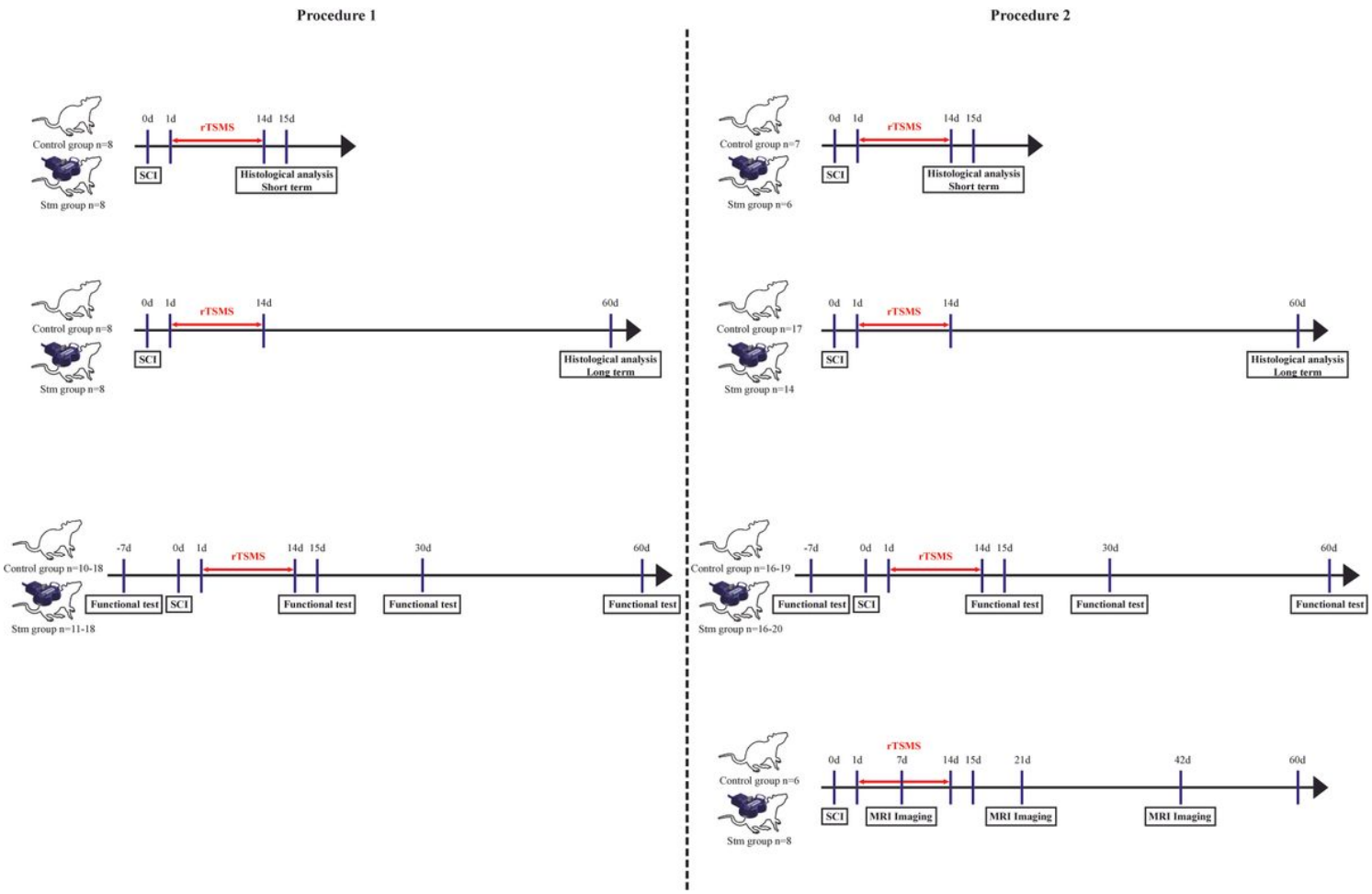

Figure 1

Experimental paradigms illustrating the timelines of the major experimental manipulations.

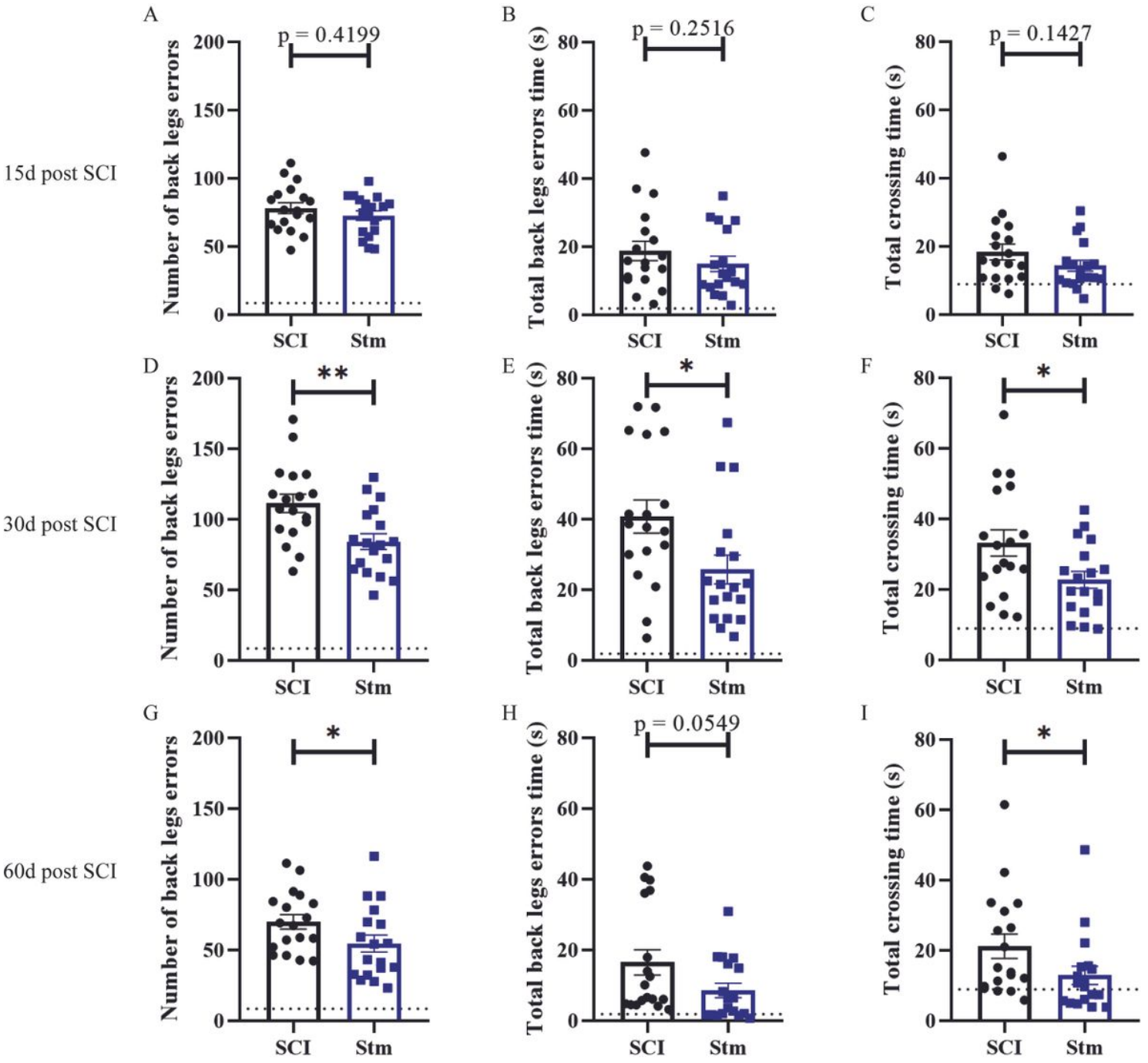

Figure 2

rTSMS treatment induces locomotor recovery after a complete transection of the spinal cord in rats. Quantification of locotronic evaluation at (A-C) 15 days, (D-F) 30 days and (G-I) 60 days after SCI. Parameters are (A, D and G) number of back legs errors, (B, E and H) total back legs errors time and (C, F and I) total crossing time. Quantifications are expressed as average ± SD. N=18 animals per group. Dashed lines correspond to the baseline parameters obtained during locotronic habituation (7 days before SCI). Quantifications are expressed as average ± SD. Statistical evaluations were based on Mann-Whitney test (* = $P < 0.05$ and ** = $P < 0.01$).

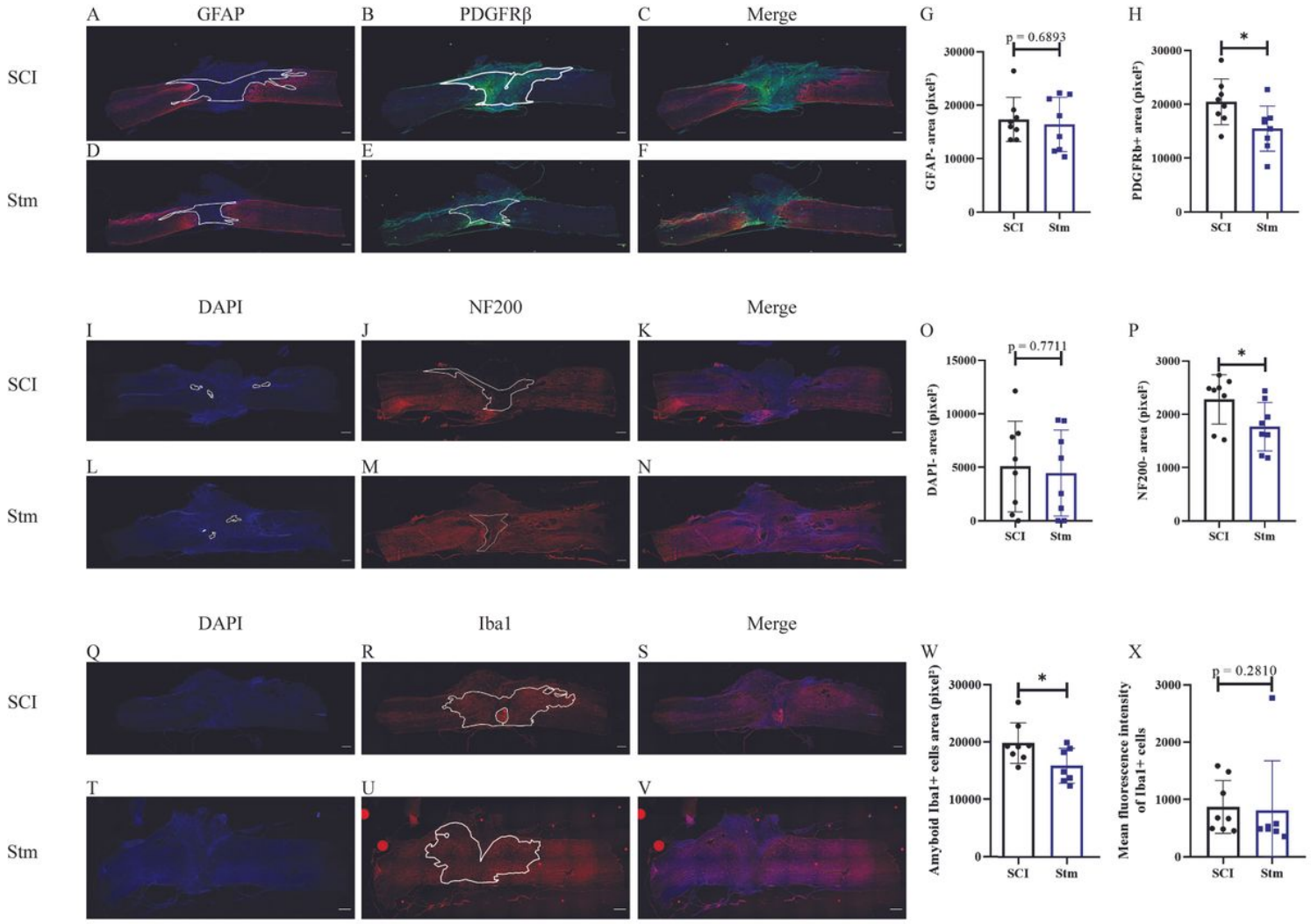

Figure 3

rTSMS treatment enhances tissue repair after a complete transection of the spinal cord 15 days after SCI in rats. At day 15 immunohistological analyses were performed. (A, B, C, D, E, F, I, J, K, L, M, N, Q, R, S, T, U and V) Representative pictures of sagittal spinal cord sections of (A, B, C, I, J, K, Q, R and S) SCI and (D, E, F, L, M, N, T, U and V) Stm (rTSMS treated) animals. Sections were stained with (A and D) GFAP, (B and E) PDGFRβ, (I, L, Q and T) DAPI, (J and M) NF200 and (R and U) Iba1. (G) Quantification of astrocytic negative area (GFAP-). (H) Quantification of fibrosis positive area (PDGFRβ+). (O) Quantification of DAPI negative area (DAPI-). (P) Quantification of NF200 negative area (NF200-). (W) Quantification of Iba1 amyboid positive cells area (Iba1+) and (X) quantification of Iba1+ mean fluorescence intensity. Scale bars are 200µm. N=8 animals per group. Quantifications are expressed as average ± SD. Statistical evaluations were based on Mann-Whitney test (* = $P < 0.05$).

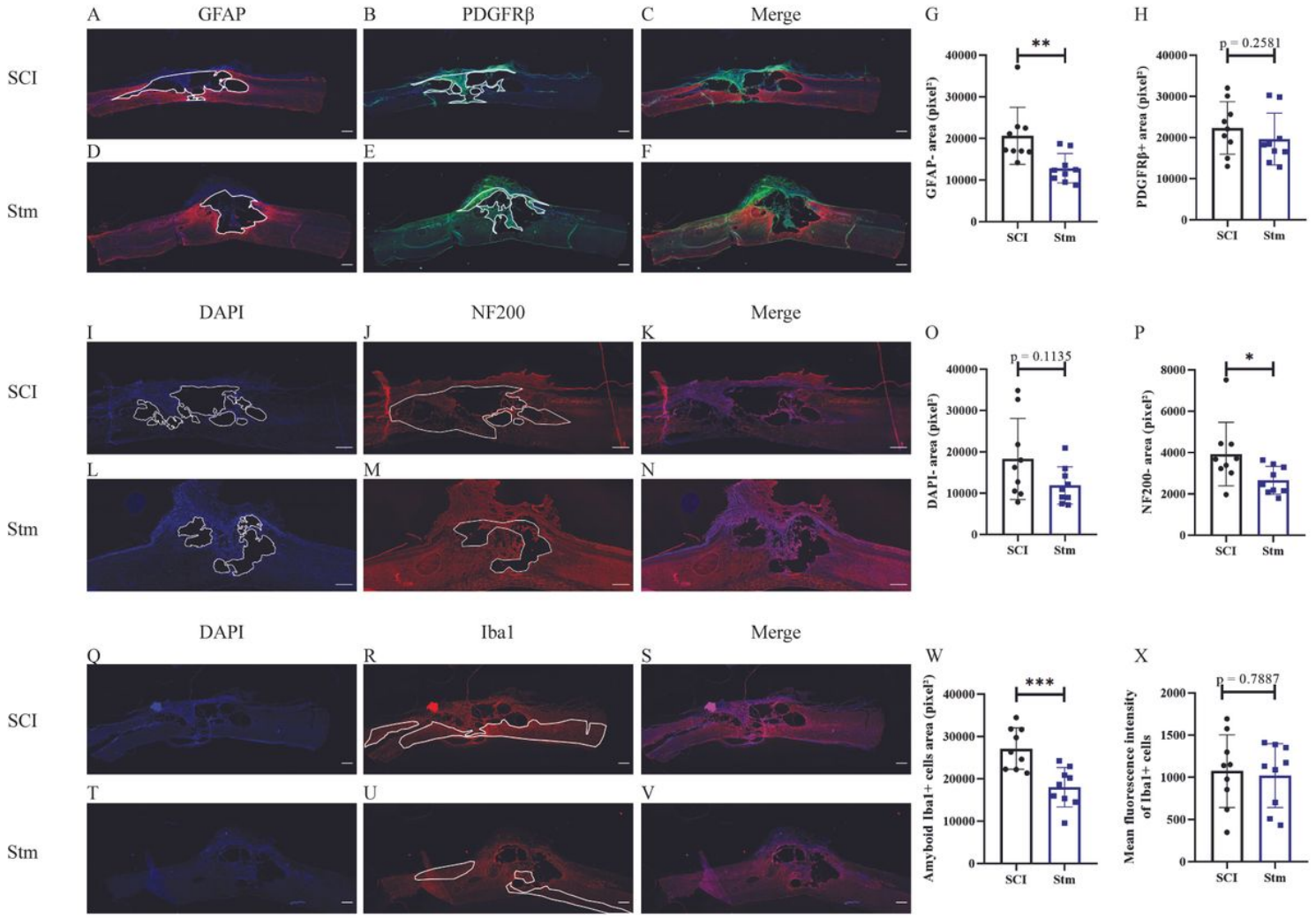

Figure 4

rTSMS treatment enhances tissue repair after a complete transection of the spinal cord 60 days after SCI in rats. At day 60 immunohistological analyses were performed. (A, B, C, D, E, F, I, J, K, L, M, N, Q, R, S, T, U and V) Representative pictures of sagittal spinal cord sections of (A, B, C, I, J, K, Q, R and S) SCI and (D, E, F, L, M, N, T, U and V) Stm (rTSMS treated) animals. Sections were stained with (A and D) GFAP, (B and E) PDGFRβ, (I, L, Q and T) DAPI, (J and M) NF200 and (R and U) Iba1. (G) Quantification of astrocytic negative area (GFAP-). (H) Quantification of fibrosis positive area (PDGFRβ+). (O) Quantification of DAPI negative area (DAPI-). (P) Quantification of NF200 negative area (NF200-). (W) Quantification of Iba1 amyboid positive cells area (Iba1+) and (X) quantification of Iba1+ mean fluorescence intensity. Scale bars are 200µm. N=8 animals per group. Quantifications are expressed as average ± SD. Statistical evaluations were based on Mann-Whitney test (* = P < 0.05, ** = P < 0.01 and *** = P < 0.001).

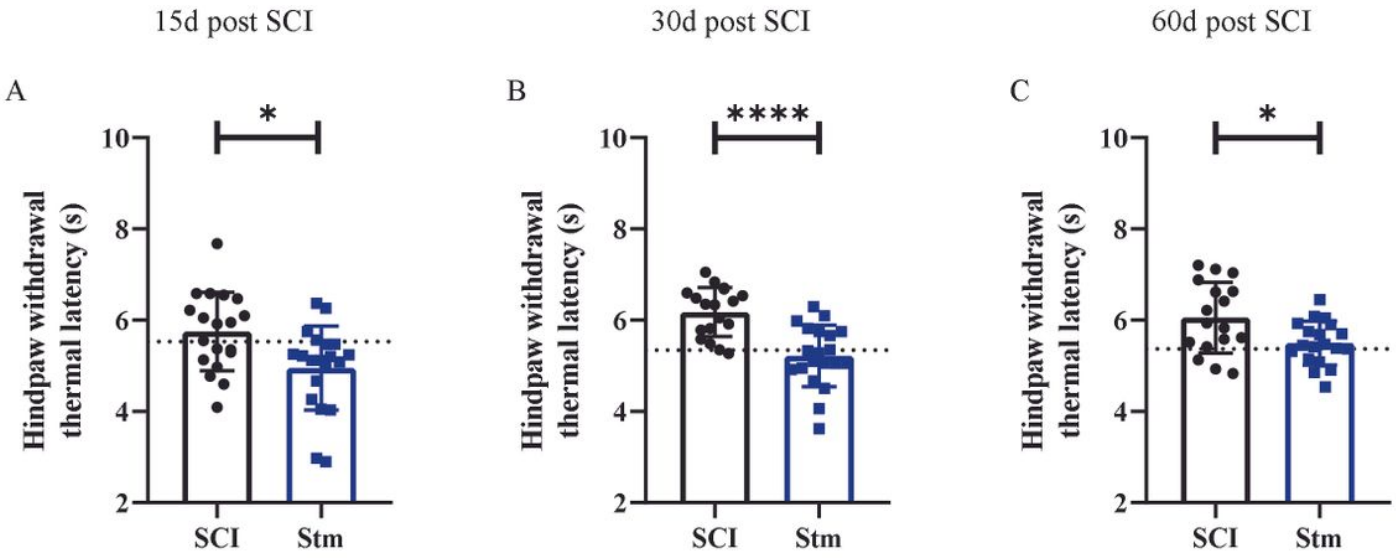

Figure 5

rTSMS treatment modulate sensitive recovery after SCI in rats. Quantification of hindpaw withdrawal thermal latency at (A) 15 days, (B) 30 days and (C) 60 days after SCI. Quantifications are expressed as average ± SD. N=19 animals per SCI group and N=20 animals per STM group at 15 days, N=18 animals per SCI group and N=20 animals per STM group at 30 days and N=17 animals per SCI group and N=19 animals per Stm group 60 days after SCI. Dashed lines correspond to the baseline parameters obtained with non-injured animals. Statistical evaluations were based on Mann-Whitney test (* = $P < 0.05$ and **** = $P < 0.0001$).

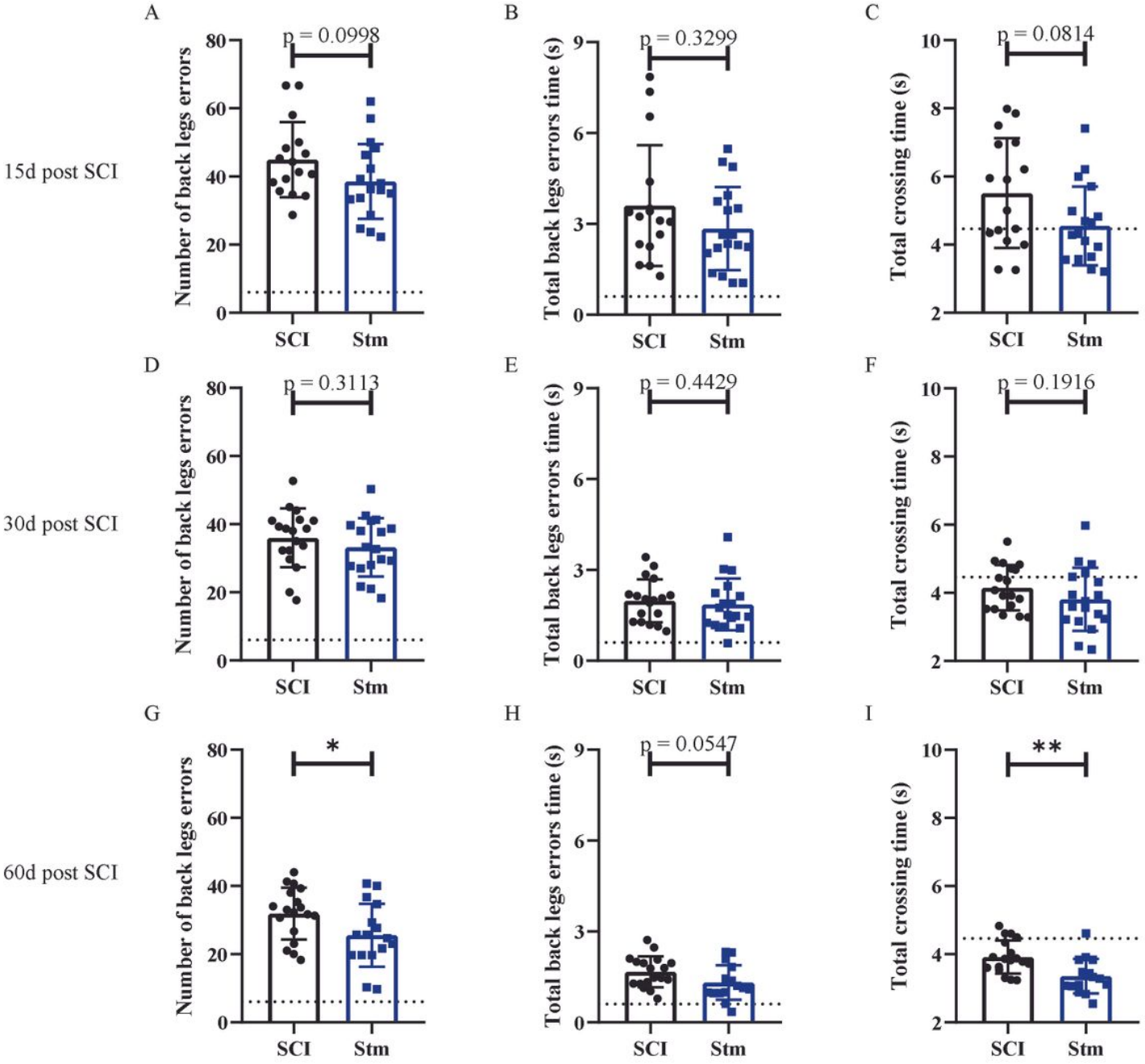

Figure 6

rTSMS treatment induces locomotor recovery after contusive SCI in rats. Quantification of locotronic evaluation at (A-C) 15 days, (D-F) 30 days and (G-I) 60 days after SCI. Parameters are (A, D and G) number of back legs errors, (B, E and H) total back legs errors time and (C, F and I) total crossing time. Quantifications are expressed as average ± SD. N=16 animals per SCI group and N=18 animals per Stm group at 15 days, N=18 animals per SCI group and N=18 animals per Stm group at 30 days and N=18 animals per SCI group and N=16 animals per Stm group 60 days after SCI. Dashed lines correspond to the baseline parameters obtained during locotronic habituation (7 days before SCI). Quantifications are expressed as average ± SD. Statistical evaluations were based on Mann-Whitney test (* = $P < 0.05$ and ** = $P < 0.01$).

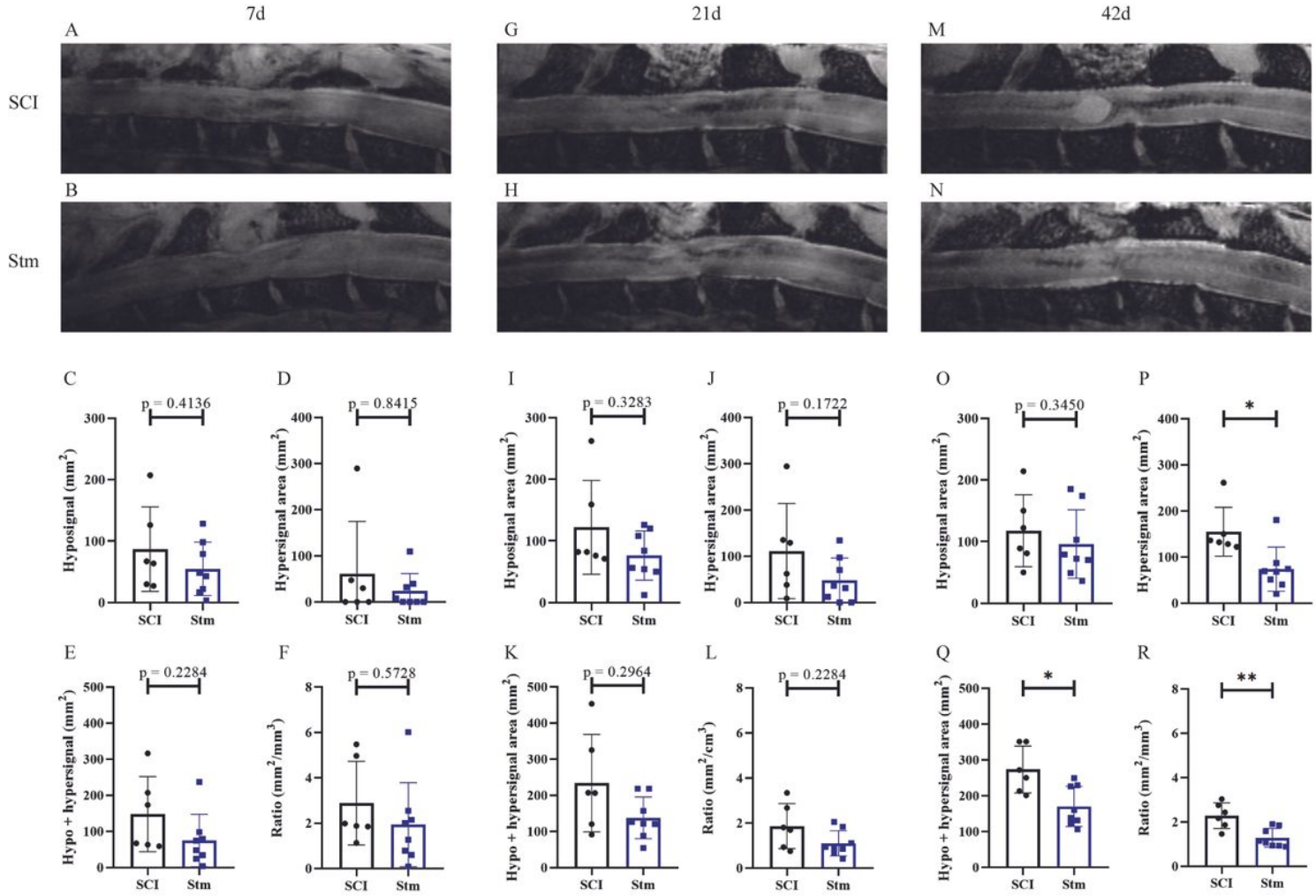

Figure 7

MRI analyses show that rTSMS treatment decreases cystic cavities and increases spinal cord spared tissue. At (A-F) 7, (G-L) 21 and (M-R) 42 days MRI experiments have been performed. Representative images of sagittal spinal cord sections recorded with MRI of (A, G and M) SCI and (B, H and N) Stm (rTSMS treated) animals. Quantification of hyposignal area (C) 7, (I) 14 and (O) 42 days after SCI. Quantification of hypersignal area (D) 7, (J) 14 and (P) 42 days after SCI. Quantification of hypo + hypersignal area (E) 7, (K) 14 and (Q) 42 days after SCI. Quantification of ratio lesioned tissue (F) 7, (L) 14 and (R) 42 days after SCI. N=6 animals per control group and N= 8 per Stm group. Quantifications are expressed as average ± SD. Statistical evaluations were based on Mann-Whitney test (* = $P < 0.05$ and ** = $P < 0.01$).

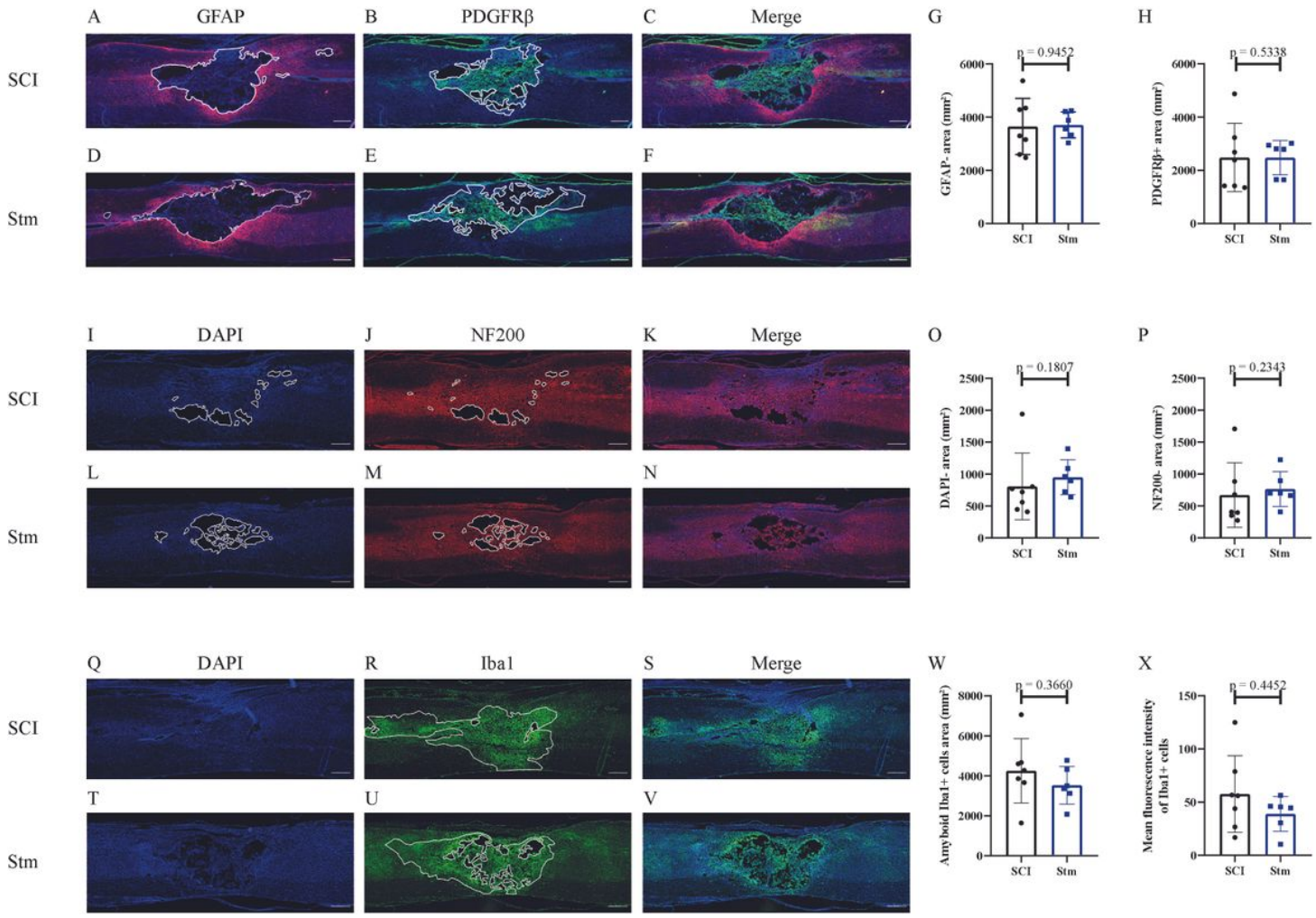

Figure 8

rTSMS treatment does not have effect on tissue repair after contusive SCI in rats 15 days after SCI. At day 15 immunohistological analyses were performed. (A, B, C, D, E, F, I, J, K, L, M, N, Q, R, S, T, U and V) Representative pictures of sagittal spinal cord sections of (A, B, C, I, J, K, Q, R and S) SCI and (D, E, F, L, M, N, T, U and V) Stm (rTSMS treated) animals. Sections were stained with (A and D) GFAP, (B and E) PDGFRβ, (I, L, Q and T) DAPI, (J and M) NF200 and (R and U) Iba1. (G) Quantification of astrocytic negative area (GFAP-). (H) Quantification of fibrosis positive area (PDGFRβ+). (O) Quantification of DAPI negative area (DAPI-). (P) Quantification of NF200 negative area (NF200-). (W) Quantification of Iba1 amyboid positive cells area (Iba1+) and (X) quantification of Iba1+ mean fluorescence intensity. Scale bars are 200µm. N=7 animals per SCI group and N=6 animals per Stm group. Quantifications are expressed as average ± SD. Statistical evaluations were based on Mann-Whitney test.

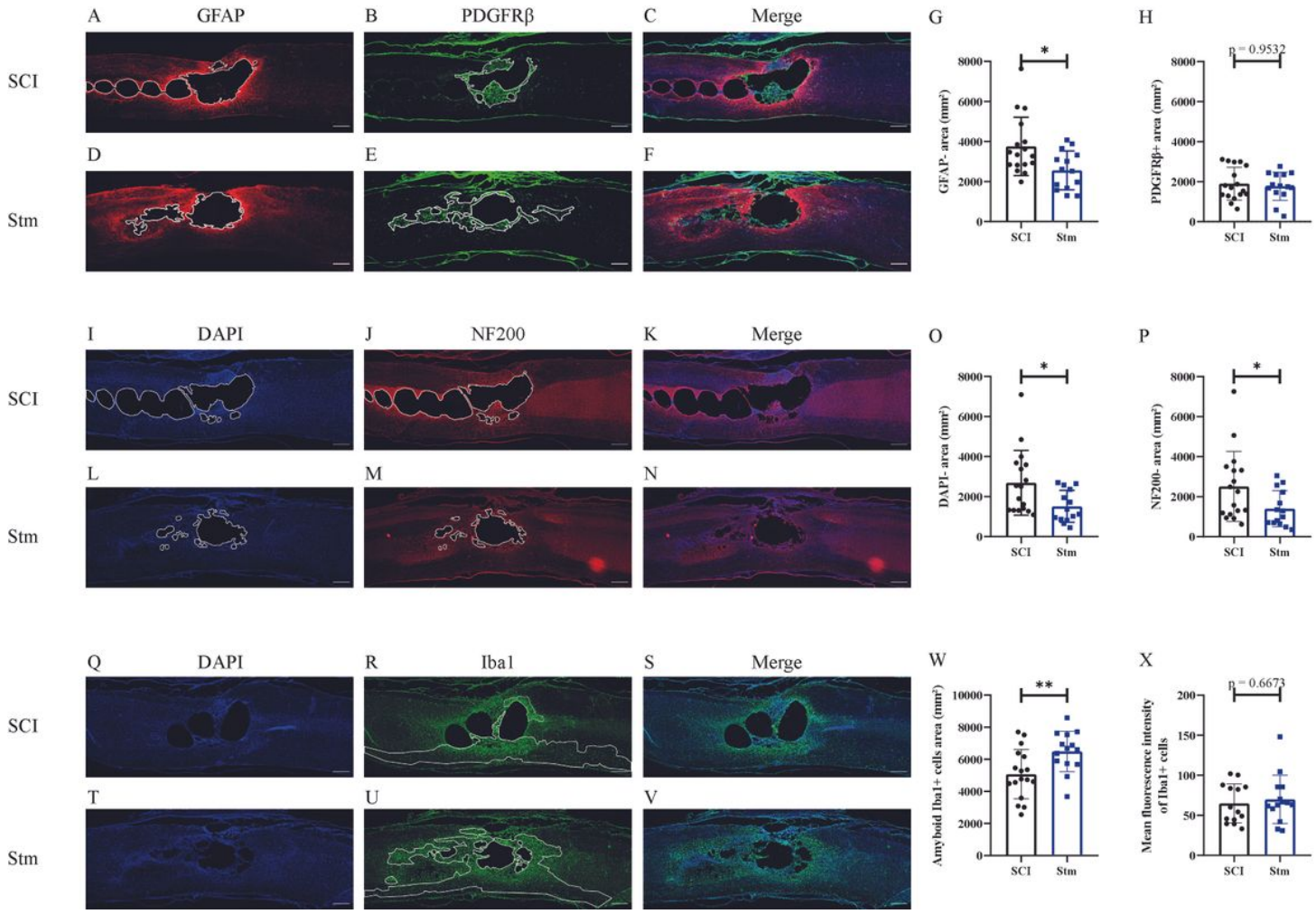

Figure 9

rTSMS treatment enhances tissue repair after contusive SCI in rats 60 days after SCI. At day 60 immunohistological analyses were performed. (A, B, C, D, E, F, I, J, K, L, M, N, Q, R, S, T, U and V) Representative pictures of sagittal spinal cord sections of (A, B, C, I, J, K, Q, R and S) SCI and (D, E, F, L, M, N, T, U and V) Stm (rTSMS treated) animals. Sections were stained with (A and D) GFAP, (B and E) PDGFRβ, (I, L, Q and T) DAPI, (J and M) NF200 and (R and U) Iba1. (G) Quantification of astrocytic negative area (GFAP-). (H) Quantification of fibrosis positive area (PDGFRβ+). (O) Quantification of DAPI negative area (DAPI-). (P) Quantification of NF200 negative area (NF200-). (W) Quantification of Iba1 amyboid positive cells area (Iba1+) and (X) quantification of Iba1+ mean fluorescence intensity. Scale bars are 200µm. N=17 animals per SCI group and N=14 per Stm group. Quantifications are expressed as average ± SD. Statistical evaluations were based on Mann-Whitney test (* = $P < 0.05$ and ** = $P < 0.01$).

Supplementary Files

This is a list of supplementary files associated with this preprint. Click to download.

- FigureS1.jpg